Exploration Geophysics (2006) ***37****, 73-85*
Butsuri-Tansa (Vol. 59, No. 1)
Mulli-Tamsa (Vol. 9, No. 1)

Theory of efficient array observations of microtremors with special reference to the SPAC method

Hiroshi Okada

Key Words: microtremor method, Rayleigh waves, Bessel functions, efficient circular array, SPAC coefficient

ABSTRACT

Array observations of the vertical component of microtremors are frequently conducted to estimate a subsurface layered-earth structure on the assumption that microtremors consist predominantly of the fundamental mode Rayleigh waves. As a useful tool in the data collection, processing and analysis, the spatial autocorrelation (SPAC) method is widely used, which in practice requires a circle array consisting of M circumferential stations and one centre station (called "M-station circle array", where M is the number of stations). The present paper considers the minimum number of stations required for a circle array for efficient data collection in terms of analytical efficacy and field effort.

This study first rearranges the theoretical background of the SPAC algorithm, in which the SPAC coefficient for a circle array with M infinite is solely expressed as the Bessel function, $J_0(rk)$ (r is the radius and k the wavenumber). Secondly, the SPAC coefficient including error terms independent of the microtremor energy field for an M-station circle array is analytically derived within a constraint for the wave direction across the array, and is numerically evaluated in respect of these error terms. The main results of the evaluation are: 1) that the 3-station circle array when compared with other 4-, 5-, and 9-station arrays is the most efficient and favourable for observation of microtremors if the SPAC coefficients are used up to a frequency at which the coefficient takes the first minimum value, and 2) that the Nyquist wavenumber is the most influential factor that determines the upper limit of the frequency range up to which the valid SPAC coefficient can be estimated.

INTRODUCTION

The desire for an exploration technique applicable to areas where conventional seismic methods are difficult or impossible to implement, such as urban or environmentally sensitive areas, has given rise to development of a method different from conventional seismic methods: the "Microtremor Survey Method" (MSM), which makes use of microtremors found in abundance anywhere on the surface of the earth (Okada, 1998, 2003; Okada et al., 1990). Typical examples of the method are the frequency-wavenumber power spectral method (referred to as the *f-k* method) (e.g., Asten and Henstridge, 1984; Horike, 1985; Matsushima and Ohshima, 1989; Matsushima and Okada, 1989, 1990; Miyakoshi et al., 1994; Yamanaka et al., 1994; Yamanaka et al., 1999), and the spatial autocorrelation method (referred to as SPAC method) (e.g., Hidaka, 1985; Hough et al., 1992; Malagnini et al., 1993; Matsuoka et al., 1996; Matsuoka and Shiraishi, 2002; Okada, 2003; Okada and Sakajiri, 1983). In recent years both versions of MSM have become of major interest as tools that could yield more quantitative information, such as shear-wave-velocity profile and thickness of sediments over seismic basement. A fundamental property common to both versions is that the microtremor is regarded as a stochastic process and its spectrum forms the basis of analysis (Okada, 2003). The seismic surface wave is a major source of information in the MSM. Because both versions observe the vertical component of microtremors, the Rayleigh wave becomes the most important of the seismic surface waves.

The *f-k* method uses the frequency-wavenumber power spectral density (*f-k* spectrum) as the statistical parameter (e.g., Capon, 1969; Lacoss et al., 1969). Its principle is to detect relatively powerful seismic waves among the microtremors. This method does not question the nature of waves, that is, whether they are dispersive or not. There is no logic in the fundamental theory of *f-k* spectral analysis with which to identify surface waves, or to judge the dispersion of the surface waves. In this sense the *f-k* method is not a way to detect surface waves specifically.

The SPAC method is based on theory developed by Aki (1957) to comprehend the relationship between the temporal and spatial spectra of seismic waves too complicated for a phase-to-phase correlation analysis (Aki et al., 1958). This theory has also formed the foundation for the SPAC method, which has become the key to successful extraction of dispersion characteristics of Rayleigh waves from microtremors. Of the MSM techniques, the SPAC method seems to be more practical and useful (Apostolidis et al., 2004; Asten, 2003, 2004; Asten et al., 2004; Chouet et al., 1998; Kudo et al., 2002; Matsuoka et al., 1996; Matsuoka and Shiraishi, 2002; Nguyen et al., 2004; Okada, 2003; Roberts and Asten, 2004, 2005; Sasatani et al., 2001).

There are few reports of the application of the SPAC method. However, it has an advantage over the *f-k* method in that it requires fewer stations and a smaller array than the *f-k* method to achieve a similar result regarding the dispersion characteristics of Rayleigh waves (Miyakoshi et al., 1996; Okada et al., 1987). The size of the array required for observation of microtremors is very important, not only because a large array increases field effort and decreases field efficiency, but also because a large array may violate the assumption required by the MSM that the layers are sub-parallel beneath the array.

A further technique for determining phase velocities of Rayleigh waves from microtremors has been developed recently by Cho et al. (2004), and this may also be included among the Microtremor Survey Methods. In their paper the emphasis lies on the theoretical development, and although the application to field data recorded at three sites is also presented, it seems to be difficult to appreciate the practical merit of their theory.

Kita 29 Nishi 7, Kita-ku
Sapporo 001-0029, Japan,
Phone & Fax: 011-716-6561
Email: hokada@sings.jp

Manuscript received August 1, 2005; accepted September 29, 2005.
Part of this paper was presented at the 104th SEGJ Conference, 2001, and published in 2002 in the Science Report of the project "Assessment of Seismic Local-Site Effects at Plural Test Sites" by coordinator Kazuyoshi Kudo supported by the Ministry of Education, Science, Sports and Culture under Research Grant No. 11694134.

In the present study, we will consider the SPAC method. Many previous workers using the SPAC method have employed a circular array, based on the fundamental theory of Aki (1957), but in practice consisting of as few as four stations. One station is at the centre of the circle and the other three are on the circumference at uniform intervals (a "3-station circle array") (e.g., Kudo et al., 2002; Matsuoka et al., 1996; Okada, 2003; Okada et al., 1990). Even where seven or ten stations are used, a combined array has been made up of two or three circular arrays of different radii with a shared centre, each of which consists of three stations arranged on the circumference at equal intervals (Kudo et al., 2002; Okada, 2003; Sasatani et al., 2001). Thus, the fundamental use of a circular array that consists of three stations on the circumference seems to be generally established in the SPAC method. However, there is doubt about whether a circular array consisting of as few as three stations on the circumference is sufficient for the application of the SPAC method. For simplicity, a circular array consisting of M stations on the circumference and one at the centre, $M + 1$ stations in total, will be referred to as "M-station circle array" hereafter.

Yamamoto et al. (1997) performed a field experiment to examine how many stations are required on the circumference of a circular array for microtremor observations to give satisfactory results for phase velocity estimation. In the experiment they examined six different circular arrays, consisting of three, four, five, six, seven, and eight stations equally spaced on the circumference around the centre station, respectively. The size of the circle ranged from 15 m to 45 m in radius. Using the SPAC method they analysed the recorded data, and found that the 3-station circle array provided phase velocities in the frequency range from 5 to 15 Hz with an error of about 5% relative to those calculated from a known shear-wave-velocity profile at the experimental site. The other circle arrays gave comparable results.

They concluded that there was no significant difference between the 3-station circle array and the other circle arrays in practical determination of phase velocities with the SPAC algorithm, and that the 3-station circle array is more practical for microtremor observations because less field effort is required. However, they gave no theoretical background to explain why a circular array with only three stations on the circumference could give a satisfactory result in phase velocity estimation.

Recently, microtremor array studies have been reported using a seven-station "hexagonal array" (Asten, 2004; Roberts and Asten, 2004) and using an alternative SPAC method, the two-site SPAC (2sSPAC) method (Morikawa et al. 2004). The hexagonal array has been used because it has the advantage of yielding independent estimates of the SPAC coefficient over four radial distances simultaneously. The 2sSPAC method has been used as a labour- and resource-saving technique in which a simultaneous observation at only two stations in a given circle array is repeated for three different directions to form an equivalent triangle array observation.

In this study we will consider comparative merits and demerits of the choice of the number of stations on a circular array and their configuration. We first rearrange the theoretical background of the SPAC algorithm, so that the logical structure of the theory may be easier to understand. Secondly, we discuss a circular array consisting of a finite number of stations, and emphasise the question of how to evaluate the efficiency of such a circular array.

SPATIAL AUTOCORRELATION COEFFICIENT

For the sake of simplicity of expression, polar coordinates (r, θ) are used.

Assumptions

We make the following assumptions about microtremors:

1. Microtremors consist of seismic plane waves coming from direction ϕ with variables of time t and position vector $\xi(r, \theta)$ (= $r(\cos\theta, \sin\theta)$), and are regarded as a stationary stochastic process both temporally and spatially. Let $X(t, \xi)$ be an observed record of the process. For $X(t, \xi)$ there exists a doubly orthogonal process $\zeta(\omega, \boldsymbol{k})$, so that $X(t, \xi)$ can be expressed in a spectral representation as

$$X(t,\boldsymbol{\xi}) = \int_{-\infty}^{\infty}\int_{0}^{\infty}\int_{0}^{2\pi} \exp\{i\omega t + i\boldsymbol{k}\boldsymbol{\xi}\}\, d\zeta(\omega,\boldsymbol{k}), \qquad (1)$$

where ω (= $2\pi f$) is the angular frequency, $\mathbf{k}$ (= $k(\cos\phi, \sin\phi)$) the wavenumber vector, and $d\zeta(\omega, \mathbf{k}) = \zeta(\omega + d\omega, \mathbf{k} + d\mathbf{k}) - \zeta(\omega,\mathbf{k})$ (Priestley, 1981).

Because the integral in this equation is defined in the mean-square sense (Priestley, 1981), the squared amplitude, $|d\zeta(\omega,\mathbf{k})|^2$, rather than $|d\zeta(\omega,\mathbf{k})|$ is important as a key term which implicitly characterises the microtremor energy field in the following analysis.

2. The process has the following property: its increments at different values of ω and $\mathbf{k}$ are uncorrelated (e.g., Yaglom, 1962; Capon, 1969; Priestley, 1981), i.e., for any two distinct sets of (ω, $\mathbf{k}$) and (ω', $\mathbf{k}'$),

   i. $E[d\zeta(\omega, \mathbf{k})] = 0$ for all ω and $\mathbf{k}$,

   ii. $E[d\zeta^*(\omega, \mathbf{k})] \cdot d\zeta(\omega', \mathbf{k}')] = dH(\omega, \mathbf{k})\delta(\omega - \omega')\delta(\mathbf{k} - \mathbf{k}')$, for any two distinct sets of (ω, $\mathbf{k}$) and (ω', $\mathbf{k}'$),

   where $E[\cdot]$ denotes an average taken over all observed records of microtremors, * the complex conjugate, $H(\omega, \mathbf{k})$ the integrated spectrum of $X(t, \xi)$, and $\delta(\cdot)$ the Dirac delta function.

3. The angular frequency ω and the wavenumber k in equation (1) are related as a function of each other, ζ, namely the microtremors expressed as a stochastic process, is significant only on the curve [ω, $k(\omega)$].

The third assumption inevitably leads to the tacit assumption that

4. the most powerful of the plane waves in microtremors is the surface wave component, and one of the surface wave modes (often the fundamental mode) is dominant.

Power spectrum of microtremors

When we discuss the vertical component of microtremors, the surface wave referred to is the Rayleigh wave. In this case, the spectral representation of equation (1) can be written as

$$X(t,r,\theta) = \int_{-\infty}^{\infty}\int_{0}^{2\pi} \exp\{i\omega t + ir k(\omega)\cos(\theta - \phi)\}\, d\zeta(\omega,\phi). \qquad (2)$$

Our main interest lies in the microtremor energy field associated with Rayleigh wave propagation, i.e., we are interested in the squared amplitude $|d\zeta(\omega,\phi)|^2$, closely related to the energy of the process, rather than in $|d\zeta(\omega,\phi)|$. It is difficult to visualise the form of the amplitudes of the random variable $d\zeta(\omega,\phi)$ as a function of frequency and direction, in equation (2). However, the total microtremor energy over the time interval (-∞, ∞) is infinite, hence

as a conventional technique we describe their spectral properties in terms of the distribution of power (i.e., energy per unit time) over a continuous range of frequencies or wavenumbers and directions in the following discussion.

In general, as spectra of microtremors are considered to be continuous and differentiable with respect to frequency and direction, the stochastic process $\zeta(\omega,\phi)$ satisfies the following relationship

$$\mathrm{E}\left[\left|d\zeta(\omega,\phi)\right|^2\right] = dH(\omega,\phi) = h(\omega,\phi)\,d\omega\,d\phi, \tag{3}$$

for which the property (ii) of the second assumption is referred to. In this equation the term $h(\omega, \phi)$, a spectral density function, may be referred to as the "frequency-direction spectrum density" (Henstridge, 1979), and $h(\omega, \phi)\,d\omega\,d\phi$ represents the average contribution to the total power from waves in $X(t, r, \theta)$ coming from the directions between ϕ and $\phi + d\phi$. with angular frequencies between ω and $\omega + d\omega$.

Integrating this average contribution over all directions, we obtain the power spectral density function (or simply the "power spectrum") of microtremors $h_0(\omega)$ at a station:

$$h_0(\omega) = \int_0^{2\pi} h(\omega,\phi)\,d\phi. \tag{4}$$

The important point to note is that the power spectrum of microtremors is not dependent on the directions to microtremor sources; that is, the power spectrum of microtremors is not dependent on whether the wave field is due to a single source or many.

SPAC function

Now, suppose there are two microtremor stations A and B a distance r apart. Let A be at the origin of the coordinate system (0, 0), and the coordinates of station B are (r, θ). From equation (2), the microtremor record at station A can be represented as

$$X(t,0,0) = \int_{-\infty}^{\infty}\int_0^{2\pi} \exp\{i\omega t\}\,d\zeta(\omega,\phi), \tag{5}$$

and the record at B as

$$X(t,r,\theta) = \int_{-\infty}^{\infty}\int_0^{2\pi} \exp\{i\omega t + irk\cos(\theta-\phi)\}\,d\zeta(\omega,\phi). \tag{6}$$

We define the spatial autocorrelation function $S(r, \theta)$, of microtremors between A and B, by

$$S(r,\theta) = \mathrm{E}\left[X^*(t,0,0)\,X(t,r,\theta)\right] = \lim_{T\to\infty}\frac{1}{2T}\int_{-T}^{T} X^*(t,0,0)\,X(t,r,\theta)\,dt, \tag{7}$$

where * denotes the complex conjugate. Using equations (3), (5), and (6), this equation reduces to

$$S(r,\theta) = \int_{-\infty}^{\infty}\left[\int_0^{2\pi}\exp\{irk\cos(\theta-\phi)\}\,h(\omega,\phi)\,d\phi\right]d\omega = \int_{-\infty}^{\infty} g(\omega,r,\theta)\,d\omega, \tag{8}$$

where

$$g(\omega,r,\theta) = \int_0^{2\pi}\exp\{irk\cos(\theta-\phi)\}\,h(\omega,\phi)\,d\phi \tag{9}$$

is the spatial covariance function ("SPAC function") that measures the covariance at frequency ω between the microtremors observed at stations A(0, 0) and B(r, θ) (Henstridge, 1979).

The SPAC function at the origin (0, 0) of the coordinate system is

$$g(\omega,0,0) = \int_0^{2\pi} h(\omega,\phi)\,d\phi, \tag{10}$$

which is identical to the power spectrum of microtremors $h_0(\omega)$ given by equation (4).

Equation (9) mathematically means that the value of SPAC function $g(\omega, r, \theta)$ depends on the frequency-direction spectrum density $h(\omega, \phi)$ which may vary within a microtremor energy field. This makes it necessary to examine whether the data observed in a specified period of time have satisfied the temporally stationary assumption. For such an examination, the power spectrum should be estimated for a number of short time segments into which the block of all data observed is divided, before performing a detailed analysis of the data, for which the direct segment, or block averaging, method (Capon, 1969) should be used.

Morikawa et al. (2004) have recently proposed the two-site SPAC (2sSPAC) method as an alternative to the SPAC method. In practice, this method depends on the SPAC function of equation (9), and implicitly relies on the assumption that the frequency-direction spectrum density $h(\omega, \phi)$ is stable throughout the period in which a series of observations is performed. If this assumption is violated, this method cannot work as an alternative to the SPAC method we consider in this paper.

AVSPAC function from averaging SPAC functions

Suppose we lay out an array that consists of an infinite number of stations placed on a circle of radius r around the origin A (the "theoretical circle array"; an array consisting of a finite number of stations placed on a circle is a "practical circle array"). We can then define the average spatial covariance function $\bar{g}(\omega,r)$ ("AVSPAC function") by averaging $g(\omega, r, \theta)$ over all directions

$$\bar{g}(\omega,r) \equiv \frac{1}{2\pi}\int_0^{2\pi} g(\omega,r,\theta)\,d\theta. \tag{11}$$

Replacing $g(\omega, r, \theta)$ by the right-hand side in equation (9) and interchanging the order of integration, we obtain

$$\bar{g}(\omega,r) = \int_0^{2\pi}\left[\frac{1}{2\pi}\int_0^{2\pi}\exp\{irk\cos(\theta-\phi)\}\,d\theta\right]h(\omega,\phi)\,d\phi. \tag{12}$$

The integral with respect to the station direction θ, in square brackets, is the Bessel function of the first kind of order zero:

$$J_0(rk) = \frac{1}{2\pi}\int_0^{2\pi}\exp\{irk\cos(\theta-\phi)\}\,d\theta. \tag{13}$$

Thus the AVSPAC function at frequency ω expressed by equation (12) can be written as

$$\bar{g}(\omega,r) = \int_0^{2\pi} J_0(rk)\,h(\omega,\phi)\,d\phi = J_0(rk)\int_0^{2\pi} h(\omega,\phi)\,d\phi, \tag{14}$$

and using equation (4), this equation simplifies to

$$\bar{g}(\omega,r) = J_0(rk)\,h_0(\omega). \tag{15}$$

Spatial autocorrelation coefficient

Now we define the spatial autocorrelation coefficient $\rho(\omega, r)$ (the "theoretical SPAC coefficient") at angular frequency ω as the AVSPAC function normalised by the power spectrum, that is,

$$\rho(\omega,r) \equiv \bar{g}(\omega,r)/h_0(\omega) = J_0(rk). \tag{16}$$

From $k = \omega/c(\omega) = 2\pi f/c(f)$, (where $c(\omega)$ or $c(f)$ is the phase velocity), equation (16) is rewritten as

$$\rho(f,r) = J_0(2\pi f r/c(f)). \tag{17}$$

Note that the theoretical SPAC coefficient thus defined is independent of factors related to the microtremor energy field such as the intensity and directional properties of waves arriving from a wide variety of sources in space and time. These factors affect the frequency-direction spectrum $h(\omega, \phi)$.

When the theoretical SPAC coefficient $\rho(f, r)$ is obtained by using a theoretical circle array of radius r, equation (17) can be solved easily for phase velocities $c(f)$ at specified frequencies. Applying an inversion technique, or a forward modelling technique to these phase velocities, a subsurface structure can be estimated immediately beneath the location of the circle array. The greater the radius of the circle array, the deeper the subsurface structure that can be estimated by that array.

It should also be added that the theoretical circle array may be regarded as an ideal array for data collection because the theoretical SPAC coefficient is not affected by spatial aliasing of the microtremor data obtained by this array.

Thus we have rearranged the theoretical background to show that a circle array can provide the theoretical SPAC coefficient as expressed by equations (16) or (17).

In actual observations, however, a practical circle array, which consists of a finite number of stations, must be used, and the SPAC coefficient estimate will be based on this. In fact, a 3-station circle array is frequently used for observations, and the resulting SPAC coefficient seems to have been incorrectly considered to be the same as the SPAC coefficient given by the theoretical circle array. Up to now, the problem of the relationship between the SPAC coefficient estimate and the number of stations to be used in the practical circle array has not been solved. A clue to the solution of the problem will be found in the AVSPAC function determined by evaluating the integral with respect to θ in equation (11). For a practical circle array, we need to reconsider this integral.

SPAC COEFFICIENT ESTIMATED FROM A PRACTICAL CIRCLE ARRAY

A practical circle array to be used for microtremor observations is made up of a finite number of stations. To such an array, however, the SPAC coefficient defined by equation (16) or (17) is not applicable, because the integral with respect to θ in square brackets in equation (12) cannot be directly replaced by the Bessel function. Fundamentally, we must reconsider the integral of the SPAC function, and replace equation (11) or (12) by a finite sum which depends on the number of stations in the practical circle array.

Let us consider an M-station circle array of radius r for $M \geq 3$. The problem here is how to express the SPAC coefficient to be estimated from such a practical circle array.

We return to the SPAC function given by equation (9), in which a function of the integrand, $\exp\{irk\cos(\theta - \phi)\}$, is the key term in question. We can rewrite this term using the Jacobi-Anger expansion (e.g., Arfken and Weber, 2001; Watson, 1952) as

$$\begin{aligned}\exp\{irk\cos(\theta-\phi)\} &= \sum_{n=-\infty}^{+\infty} \exp\{in\pi/2\} J_n(rk) \exp\{in(\theta-\phi)\} \\ &= J_0(rk) + 2\sum_{n=1}^{\infty} i^n J_n(rk)\cos\{n(\theta-\phi)\},\end{aligned} \tag{18}$$

where $J_n(rk)$ is the Bessel function of the first kind of order n.

Using this expansion, we approximate the integral with respect to θ in equation (11) or (12) with a finite sum of its integrand up to M, the number of stations on the circle. The AVSPAC function for the M-station circle array $\hat{g}(M;\omega,r)$ corresponding to $\bar{g}(\omega,r)$ in equation (11) or (12) may now be expressed as

$$\begin{aligned}\hat{g}(M;\omega,r) = &\frac{1}{2\pi}\sum_{j=1}^{M} J_0(rk)\Delta\theta_j \int_0^{2\pi} h(\omega,\phi)\,d\phi \\ &+ \frac{1}{2\pi}\sum_{j=1}^{M}\left\{\int_0^{2\pi} 2\sum_{n=1}^{\infty}\Phi(n;rk,\alpha_j)\,h(\omega,\phi)\,d\phi\right\}\Delta\theta_j,\end{aligned} \tag{19}$$

where

$$\Phi(n;rk,\alpha_j) = J_{2n}(rk)\cos 2n\alpha_j + iJ_{2n-1}(rk)\sin(2n-1)\alpha_j,$$

$$\alpha_j = \pi/2 - (\theta_j - \phi) \quad \text{for} \quad j = 1,2,\ldots,M,$$

and $\Delta\theta_j$ is the direction interval between the jth and $(j+1)$th stations.

If M stations are placed on the circumference at equal intervals, then $\Delta\theta_j = \Delta\theta = 2\pi/M$, and we can write

$$\sum_{j=1}^{M}\Delta\theta_j = M\Delta\theta = 2\pi.$$

The real part of the AVSPAC function, $\mathrm{Re}[\hat{g}(M;\omega,r)] \equiv \hat{g}_M(\omega, r)$, being observable, may be written as

$$\begin{aligned}\hat{g}_M(\omega,r) = &J_0(rk)\,h_0(\omega) \\ &+ \int_0^{2\pi}\frac{1}{M}\sum_{j=1}^{M}\left\{2\sum_{n=1}^{\infty}J_{2n}(rk)\cos 2n\alpha_j\right\}h(\omega,\phi)\,d\phi,\end{aligned} \tag{20}$$

or from $\alpha_j = \pi/2 - (\theta_j - \phi)$

$$\begin{aligned}\hat{g}_M(\omega,r) = &J_0(rk)\,h_0(\omega) + 2\sum_{n=1}^{\infty}(-1)^n J_{2n}(rk) \\ &\times\int_0^{2\pi}\frac{1}{M}\sum_{j=1}^{M}\cos\{2n(\theta_j-\phi)\}h(\omega,\phi)\,d\phi.\end{aligned} \tag{21}$$

The summation over j, for n and ϕ given, in equation (21) varies depending on the number of stations M and on M being either even or odd; for M odd

$$\sum_{j=1}^{M}\cos\{2n(\theta_j-\phi)\} = \begin{cases} M\cos\{2lM(\theta_1-\phi)\}, & n = lM, \\ 0, & n \neq lM, \end{cases} \tag{22}$$

and for M even

$$\sum_{j=1}^{M}\cos\{2n(\theta_j-\phi)\} = \begin{cases} M\cos\{lM(\theta_1-\phi)\}, & n = lM/2, \\ 0, & n \neq lM/2, \end{cases} \tag{23}$$

respectively, where $l = 1, 2, 3, \ldots$ in each equation.

If we choose the coordinate origin so that $\theta_1 = 0$, equation (21) becomes

$$\hat{g}_M(\omega,r) = J_0(rk)\,h_0(\omega) + 2\sum_{l=1}^{\infty}(-1)^{\nu l M} J_{2\nu l M}(rk) \times \int_0^{2\pi} \cos\{2\nu l M\phi\}\,h(\omega,\phi)\,d\phi, \quad (24)$$

where $\nu = 1$ for M odd, and $\nu = ½$ for M even. The integral in the second term represents factors related to the microtremor energy field, such as the intensity and directional properties of waves arriving from a variety of sources. In these factors the function $\cos(2\nu l M\phi)$ plays a key role in detecting the direction of arriving waves by an M-station circle array.

Using the mean value theorem, the integral in equation (24) becomes

$$\int_0^{2\pi} \cos(2\nu l M\phi)\,h(\omega,\phi)\,d\phi = \cos(2\nu l M\phi_\xi)\int_0^{2\pi} h(\omega,\phi)\,d\phi = \cos(2\nu l M\phi_\xi)\,h_0(\omega), \quad (25)$$

where $\nu = 1$ for M odd, and $\nu = ½$ for M even. The function $\cos(2\nu l M\phi_\xi)$ is bounded as

$$0 \le \left|\cos(2\nu l M\phi_\xi)\right| \le 1, \quad (26)$$

for all M and in the interval $0 \le \phi_\xi \le 2\pi$. Note that this function, representing the coefficient of the Bessel function in the series in equation (24), plays a role in reducing the magnitude of the corresponding term.

Thus the AVSPAC function in equation (24) may be rewritten as

$$\hat{g}_M(\omega,r) = J_0(rk)\,h_0(\omega) + 2\sum_{l=1}^{\infty}(-1)^{\nu l M} J_{2\nu l M}(rk)\cos(2\nu l M\phi_\xi)\,h_0(\omega), \quad (27)$$

where $\nu = 1$ for M odd, and $\nu = ½$ for M even.

Now we define the SPAC coefficient $\hat{\rho}_M(\omega,r)$ at frequency ω depending on the number of stations M as

$$\hat{\rho}_M(\omega,r) \equiv \hat{g}_M(\omega,r)\big/h_0(\omega), \quad (28)$$

which can be expressed corresponding to equation (24) as

$$\hat{\rho}_M(\omega,r) = J_0(rk) + 2\sum_{l=1}^{\infty}(-1)^{\nu l M} J_{2\nu l M}(rk)\cos(2\nu l M\phi_\xi), \quad (29)$$

where $\nu = 1$ for M odd, and $\nu = ½$ for M even.

The SPAC coefficient thus defined can be determined only after every direction ϕ_ξ of plane waves propagating across the array is specified. In practice, however, it is almost impossible to specify all ϕ_ξ values, because ϕ_ξ is a random variable and an algorithm to study such source factors has not yet been developed for the SPAC method under discussion.

The behaviour of the averaged coherency, which is equivalent to the SPAC coefficient defined in equation (29), has been studied by Asten (2003) and Asten et al. (2004). For example, Asten (2003) studied a numerical model of single pair, triangular, hexagonal and square arrays. Plane waves crossing the array with uniform amplitudes were restricted to a range of azimuths ϕ, i.e., ϕ = 30°, 60°, and 90°. The result he provided, on the variation of the real and imaginary parts of the averaged coherency due to changes in microtremor source factors, is worthy of note. Asten also obtained the result that the triangular or hexagonal arrays provide adequate azimuthal averaging coherency for application of the SPAC method, which may be helpful when devising an efficient circular array. For details, see Asten (2003) and Asten et al. (2004).

Asten (2005) further discussed the practically obscure but theoretically important role of the imaginary component of the coherency in detecting departures from plane-wave stationarity due to changes in the wavefield across the array, or local lateral variations in geology beneath the array.

Although the microtremor source factors examined in Asten (2003) and Asten et al. (2004) may be unrealistic and are restricted to a few cases from an infinite number of possibilities, their studies certainly make up for our lack of investigation into the influence of microtremor source factors. However, we believe that even if we pursue questions about microtremor source factors, it will be impossible to find an appropriate answer: our present purpose is only to consider comparative merits and demerits for the number of stations on a circle, and their configuration.

Returning to equation (26), we take an upper limit on the function $\cos(2\nu l M\phi_\xi)$ as a constraint equation, in which ϕ_ξ represents a "bound variable". Thus

$$\cos(2\nu l M\phi_\xi) = 1, \quad (30)$$

where $\nu = 1$ for M odd, and $\nu = ½$ for M even, so that the SPAC coefficient to be derived for any M in the following procedure may be constrained to one which deviates most from the theoretical SPAC coefficient as defined in equation (16). In the absence of constraints, the function $\cos(2\nu l M\phi_\xi)$ reduces the magnitude of the corresponding term in the infinite sum in equation (29), depending on the values of M and ϕ_ξ. For the present purpose, we take the equation of constraint (30) to be a reasonable compromise.

Tentatively solving the equation of constraint (30) for the bound value ϕ_ξ, the direction of waves propagating across the M-station circle array, we obtain

$$\phi_\xi = n\pi/\nu l M, \quad \text{for } n = 0, 1, 2, \ldots, \quad (31)$$

where again $\nu = 1$ for M odd, and $\nu = ½$ for M even. As an example, consider a 3-station circle array. Then $M = 3$ ($\nu = 1$), and for $l = 1$ in this equation we obtain the directions of waves predominantly propagated through the array as ϕ_ξ = 0, π/3, 2π/3, ... , 5π/3, for n = 0, 1, 2, ... , 5, respectively. These correspond to the directions between station pairs in the 3-station circle array. For the present purpose it is not worth while examining other solutions more closely.

Using equations (29) and (30) we obtain the SPAC coefficient estimated from a practical circle array as

$$\hat{\rho}_M(\omega,r) = J_0(rk) + 2\sum_{l=1}^{\infty}(-1)^{\nu l M} J_{2\nu l M}(rk), \quad (32)$$

where $\nu = 1$ for M odd, and $\nu = ½$ for M even.

Like the theoretical SPAC coefficient in equation (16) or (17), the SPAC coefficient thus obtained is independent not only of the direction of microtremors arriving at the array ϕ, but also of the power of the microtremor energy sources.

An important point to note from equations (29) and (32) is that the SPAC coefficient for $M = 4m+2$ is the same as that for $M = 2m+1$, that is,

$$\hat{\rho}_{4m+2}(\omega,r) = \hat{\rho}_{2m+1}(\omega,r). \quad (33)$$

This may easily be verified by substituting $4m+2$ for M and ½ for ν in equation (32) or (29). For example, when $M = 6$, which forms a hexagonal array, equation (33) gives $\hat{\rho}_6(\omega,r) = \hat{\rho}_3(\omega,r)$ but this is a natural result because of the spatial stationarity assumed for microtremors observed in a given array; that is, the SPAC function defined in equation (9) for the microtremors observed at the centre of a circular array and a site (r, θ) on a circle of radius r must essentially be equal to the SPAC function for the microtremors observed at the centre and another site on the opposite side of the same circle $(r, \theta \pm \pi)$.

The assumption of spatial stationarity also allows us to suggest that a circular array may be superseded by a semi-circular array (Aki, 1965; Asten et al., 2004; Okada et al., 2003). This is because if M in equations (32) or (29) is even, and such that $M = 4m$ where $m \geq 2$, or $M = 4m + 2$ where $m \geq 1$, then the SPAC coefficient expressed by equations (32) or (29) must be equal to the SPAC coefficient from the semi-circular array that consists of half of the M stations, that is, $2m$ or $2m + 1$ stations on the semi-circumference, and one at the centre. Asten et al. (2004) show examples of modelled SPAC spectra (referred to as SPAC coefficients in this paper) for a semi-circular array.

Asten et al. (2004) describe a situation in which a triangle-based array was replaced by a semi-circular array. Following from this example, it is proposed that a semi-circular array might be applied to a modified "profile line survey", along a set of parallel straight or zigzag lines such as are employed by the conventional seismic surveying method. This possibility contrasts with the current use of a circular array, which is generally restricted to a "point survey" at a specific location.

In equation (32), the second term, an infinite sum of Bessel functions, may be regarded as the error in the SPAC coefficient arising from the use of an M-station circle array. Using $\varepsilon_M(rk)$ to represent this "error term", the error term may be written as

$$\varepsilon_M(rk) = 2\sum_{l=1}^{\infty}(-1)^{\nu l M} J_{2\nu l M}(rk), \quad (34)$$

where $\nu = 1$ for M odd, and $\nu = ½$ for M even.

We observe that the SPAC coefficient defined by equation (32) is conveniently independent of the direction of arrival of microtremors at the array because of the use of the constraint equation (30). Although the SPAC coefficient depends on the behaviour of the Bessel functions for two variables (array radius r and wavenumber k), the number of stations plays a very important role in determining the integral order of each Bessel function, and the sign of coefficients, in the error term. We now consider the magnitude of the error term as it is defined here.

EVALUATION OF THE ERROR TERM OF SPAC COEFFICIENT

We consider the error term in the SPAC coefficient defined for an M-station circle array.

The error term in equation (34) may be considered to have two contributions. One contribution consists of terms due to the finite number of stations in the practical circle array; the second contribution relates to the constraint equation (30), which deals with the direction of approach of microtremor waves. The measurement error accompanying the estimation of the SPAC coefficient must basically be less than the error term defined in equation (34). Of these contributions the former is the subject of our present interest.

The error term has the property that signs in the summation are either always positive, or alternate between positive and negative depending on the number of stations. This seems to imply the possibility of constructive interference or partial cancellation between the terms depending on the chosen value of M and the wavenumbers concerned.

Keeping this possibility in mind, we evaluate the error term of the SPAC coefficient as a function of the number of stations. For this evaluation, neither wavenumber k nor array radius r is taken as an individual variable, but the product of array radius and wavenumber rk, the argument of the Bessel function, is instead taken as an independent variable and is referred to as "wavenumber" here.

For this evaluation, let us consider four different circular arrays: 3-, 4-, 5-, and 9-station circle arrays. The 3-station circle array has frequently been used for observations, and so may be considered as a typical circular array and to have the minimum number of stations. The 4-station circle array is easier to arrange on a given area, and therefore reduces field effort, as Asten (2003) has observed. There are few case studies in which 5- and 9-station circle arrays have been used, but the 5-station circle array may be regarded as an example of a practical circular array with a moderate number of stations, and the 9-station circle array as an extreme example of a practical circular array. Expanding equation (32) with the appropriate substitutions for each array, we find

$$\hat{\rho}_3(\omega,r) = J_0(rk) + 2\left[-J_6(rk) + J_{12}(rk) - J_{18}(rk) + \cdots\right], \quad (35a)$$

$$\hat{\rho}_4(\omega,r) = J_0(rk) + 2\left[J_4(rk) + J_8(rk) + J_{12}(rk) + \cdots\right], \quad (35b)$$

$$\hat{\rho}_5(\omega,r) = J_0(rk) + 2\left[-J_{10}(rk) + J_{20}(rk) - J_{30}(rk) + \cdots\right], \quad (35c)$$

$$\hat{\rho}_9(\omega,r) = J_0(rk) + 2\left[-J_{18}(rk) + J_{36}(rk) - J_{54}(rk) + \cdots\right], \quad (35d)$$

The quality of the SPAC coefficient as given in equations (35a) to (35d) may be measured by the magnitude of error term, together with the extent of the wavenumber range in which valid SPAC coefficients can be estimated while minimising this error term. If we neglect the possibility of partial interference between the Bessel functions concerned in the error term, the above equations appear to provide valid SPAC coefficients to be expected in a wavenumber range that extends as the number of stations increases. For this evaluation, either the absolute value or the relative value of the error term at relevant wavenumbers could be examined. The relative value of the error term, $\varepsilon_M(rk)/J_0(rk)$, is however inadequate, because if rk is such that $J_0(rk)$ is near an axis crossing (highly probable in practice), then the ratio may become very large. Hence, we prefer the absolute value of the error term. Since the value of $\hat{\rho}(\omega,r)$ can be obtained from observed data within the range $|\hat{\rho}(\omega,r)| \leq 1$ to two decimal places (of which, however, the hundredths place is probably uncertain), as a practical criterion we use a value of 10^{-2} as a tolerance on the absolute value of $\varepsilon_M(rk)$.

We define the "deviation wavenumber" rk_d, as the lowest value of rk at which the absolute value of $\varepsilon_M(rk)$ is on the verge of exceeding the specified tolerance of 10^{-2}.

For a 3-station circle array, the error term in equation (35a) is shown in Figure 1(b) together with the first three contributions. Looking at the behaviour of the error term in the figure, the partial cancellation due to the alternating signs of the contributing functions does not seem to take place in the range of wavenumbers shown, but interference between the first two functions does occur around $rk = 13$. Figure 1(c) shows the SPAC coefficient, including the error term, compared with the theoretical SPAC coefficient.

The dominant contribution to the error term is twice the Bessel function of order six, $2J_6(rk)$. As shown in Figure 1(c), the deviation wavenumber for this contribution is $rk_d \approx 2.58$, beyond which the difference between the SPAC coefficients for the 3-station circle array and the theoretical SPAC coefficient becomes clearly discernible. In the figure, we also note that the deviation wavenumber thus obtained is very near the wavenumber $rk_m \approx 3.83$ at which the theoretical SPAC coefficient takes its first minimum value.

For a 4-station circle array, the error term in equation (35b) is shown in Figure 2(b) together with the first three contributions. We see the error term becomes large and positive value for $2 < rk < 13$, which is caused by the term $2J_4(rk)$ dominating in $2 < rk < 7.5$, and the interference between the first three functions in the error term occurring around $rk = 12$. Figure 2(c) compares the SPAC coefficient, including the error term, with the theoretical SPAC coefficient. The dominant term $2J_4(rk)$ in the error term results in a very low deviation wavenumber, $rk_d \approx 1.20$; wavenumbers for which the SPAC coefficient are expected to be valid are limited to an extremely narrow wavenumber range. This allows us to suggest that the 4-station circle array is unsuitable for a practical circle array.

Figures 3 and 4 show the layouts and error terms for 5- and 9-station circle arrays, respectively, using equations (35c) and (35d). The SPAC coefficients are compared with the theoretical SPAC coefficient in Figures 3(c) and 4(c).

The dominant contributions in the error terms are $2J_{10}(rk)$ for a 5-station circle array and $2J_{18}(rk)$ for a 9-station circle array; the deviation wavenumber corresponding to each dominant term is $rk_d \approx 5.77$ and $rk_d \approx 12.78$, near which the theoretical SPAC coefficient reaches its second zero, for the 5-station circle array, and the fourth zero, for the 9-station circle array, respectively. As is evident from these figures, the wavenumber range over which valid SPAC coefficients can be expected extends as the number of stations increases.

The deviation wavenumbers for practical circular arrays with 3 to 10 circumferential stations are summarised in Figure 5. The deviation wavenumber in general increases with the number of stations, thus extending the wavenumber range for which valid SPAC coefficients are available. However, arrays consisting of an odd number of stations, for example $M = 3$ or 5, provide the same deviation wavenumber as arrays with twice the number of stations (e.g., $M = 6$ or 10), as expected from equation (33), which implies that the latter is less efficient than the former for field work and data analysis as well.

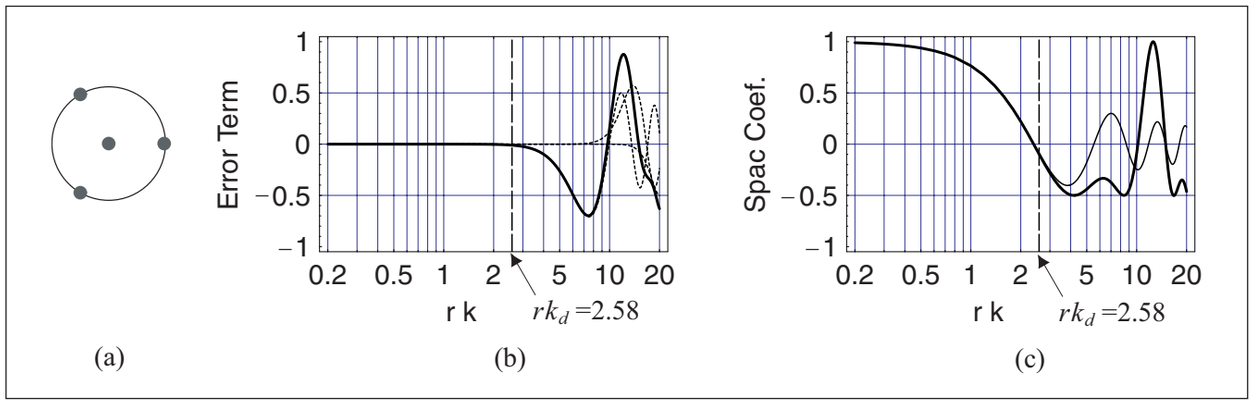

Fig. 1. SPAC coefficient for a 3-station circle array of radius r, and its error term. (a) Array configuration of a 3-station circle array. (b) Error term of SPAC coefficient (thick solid line). Dotted lines are the first three error terms, $-2J_6(rk)$, $2J_{12}(rk)$, and $-2J_{18}(rk)$. (c) SPAC coefficient for a 3-station circle array (thick solid line) and that for a theoretical circle array (thin solid line). All curves coincide for $rk < rk_d$, where rk_d is the deviation wavenumber (dashed line).

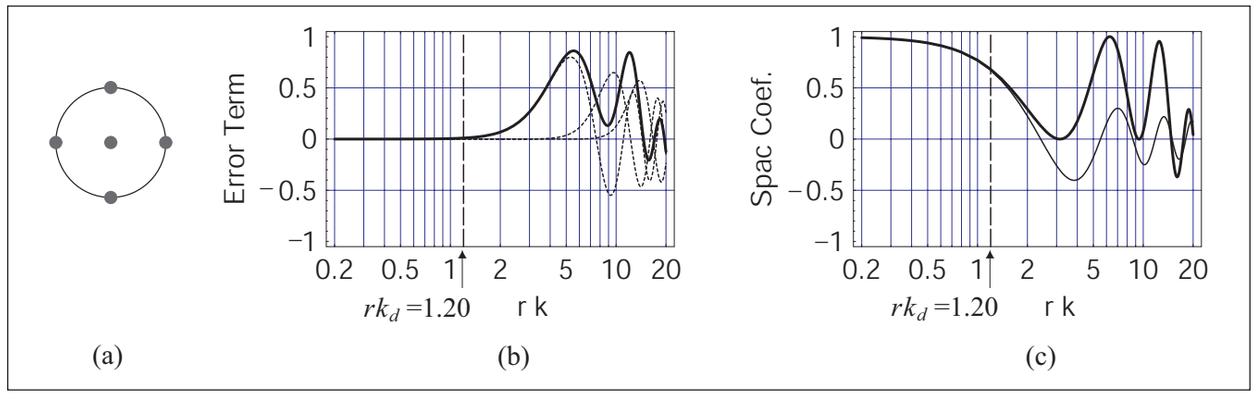

Fig. 2. SPAC coefficient for a 4-station circle array of radius r, and its error term. (b) Dotted lines are the first three error terms, $2J_4(rk)$, $2J_8(rk)$, and $2J_4(rk)$. See Figure 1 for additional details.

Comparison of the SPAC coefficients obtained from practical and theoretical circle arrays shows that the number of stations plays a role in setting a limit to the wavenumber (rk_d) which determines limit up to which the circle array provides valid SPAC coefficients. This also shows that increasing the number of stations extends the wavenumber range for valid SPAC coefficients. The use of an odd number of stations in the circle array is more efficient than the use of an even number.

DISCUSSION

The range of validity of SPAC coefficients, as estimated from observations made with a practical M-station circle array, has been evaluated by the criterion of the deviation wavenumber. After a numerical examination for 3-, 4-, 5-, and 9-station circle arrays, it seems reasonable to propose that the 3-station circle array is the most efficient among those, if the SPAC coefficient is to be evaluated up to the wavenumber, or equivalently the frequency, around which the coefficient takes its first minimum value. With our evaluation, we must further refer to the discussion of errors in SPAC coefficients by Henstridge (1979) and Matsuoka et al. (1996).

Error of SPAC coefficient for an M-station circle array

Referring to estimates of the averaged complex coherence from observations made with a circular array, Henstridge (1979) stated that the wavenumber rk to be used for analysis must lie in the range from 0.4 to 3.2, or alternatively the wavelengths must lie between $2r$ and $15r$ (r is the radius of the array), because the errors in $J_0(rk)$ are greatly magnified outside this range. His statement is based on the evaluation of the variance of an estimated wavenumber $\hat{k}(\omega)$ at angular frequency ω. If an estimate $\hat{\rho}(\omega,r)$ of the averaged coherence is very close to its maximum or minimum, the estimate $\hat{k}(\omega)$ for the $\hat{\rho}(\omega,r)$ will have large variance, which in turn introduces a large error into the corresponding phase velocities.

On the other hand, Matsuoka et al. (1996) discussed small perturbations of the averaged coherence $\hat{\rho}(\omega,r)$ obtained by a circular array, which affects the estimated wavenumber $r\hat{k}$ and therefore provides a small change in phase velocity. A key equation they discussed is

$$dx/d\rho(x) = -1/J_1(x) \tag{36}$$

where $x(=r\hat{k}) = r\omega/c$ is the wavenumber (c is the phase velocity). This equation can be derived from equation (16), where the SPAC coefficient is defined for a theoretical circle array.

We also will consider the case where a small change in phase velocity δc is due to the error $\delta\rho_M$ in the SPAC coefficient resulting from the M-station circle array employed. The key equation corresponding to equation (36) may be written as

$$\begin{aligned}\delta c &= \left|\left(\frac{\partial c}{\partial \hat{\rho}_M(x)}\right)_\omega\right|\delta\rho_M = \left|\left(\frac{\partial c}{\partial x}\right)_\omega\left(\frac{\partial x}{\partial \hat{\rho}_M(x)}\right)_\omega\right|\delta\rho_M \\ &= \left|\frac{c}{x}\cdot\frac{1}{\hat{\rho}'_M(x)}\right|\delta\rho_M,\end{aligned} \tag{37}$$

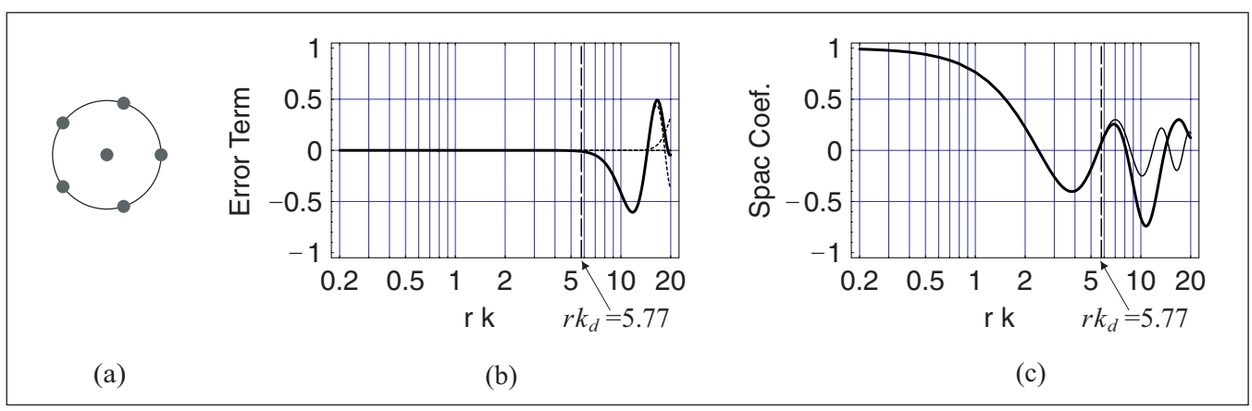

Fig. 3. SPAC coefficient for a 5-station circle array of radius r, and its error term. (b) Dotted lines are the first three error terms, $-2J_{10}(rk)$, $2J_{20}(rk)$, and $-2J_{30}(rk)$. The third term ($-2J_{30}(rk)$) is insignificant for $rk < 20$. See Figure 1 for additional details.

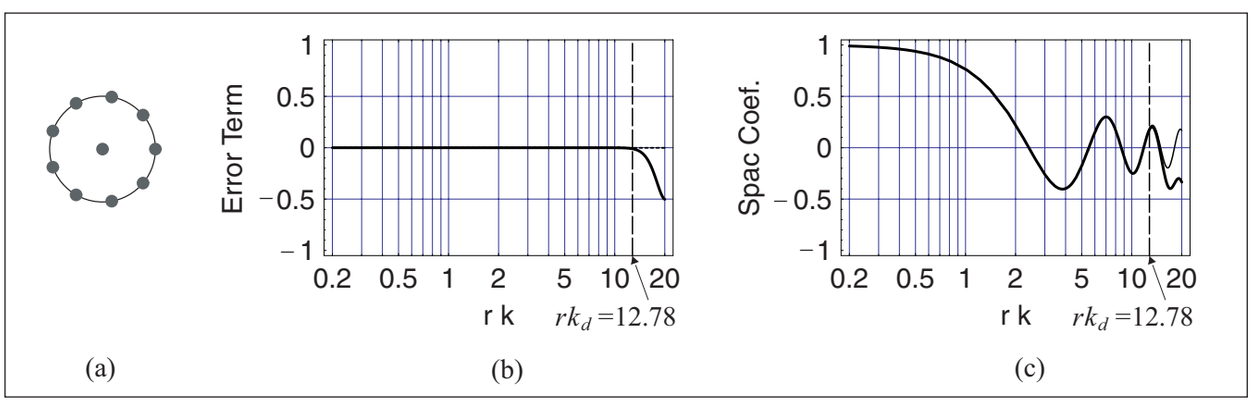

Fig. 4. SPAC coefficient for a 9-station circle array of radius r, and its error term. (b) Dotted lines are the first three error terms, $-2J_{18}(rk)$, $2J_{36}(rk)$, and $-2J_{54}(rk)$. See Figure 1 for additional details.

where $x = rk$, the wavenumber. For convenience, let us call the function $\left|1/\hat{\rho}'_M(x)\right|$ in this equation the "influence function" and denote it by $|\Delta(x)|$, which may be written, using equations (32) and (34), as

$$\left|\Delta(x)\right| \equiv \left|\frac{1}{\hat{\rho}'_M(x)}\right| = \left|\frac{\partial}{\partial x}\left[J_0(x) + \varepsilon_M(x)\right]\right|^{-1} = \left|-J_1(x) + \varepsilon'_M(x)\right|^{-1}, \quad (38)$$

where

$$\varepsilon'_M(x) = \sum_{l=1}^{\infty}(-1)^{\nu l M}\left[J_{2\nu l M-1}(x) - J_{2\nu l M+1}(x)\right], \quad (39)$$

where $\nu = 1$ for M odd, and $\nu = ½$ for M even.

Equation (38) corresponds to equation (36) derived for the theoretical circle array.

Figure 6 shows the influence function $|\Delta(x)|$ calculated for practical circle arrays (each lower diagram), to which the practical and theoretical SPAC coefficients, shown in Figures 1 to 4, are also attached for comparison (each upper diagram). The deviation wavenumber rk_d for each practical circle array and the wavelength range, $15r > \lambda > 2r$, corresponding to wavenumber range, $0.4 < rk < 3.2$, assigned by Henstridge (1979) are also shown in the figure.

From Figure 6 we can read the solution to the question of how to assign the upper limit of the wavenumber range up to which the SPAC coefficient can be estimated with the minimum effect of the error term and influence function. The solution, depending on the number of stations in the array, is that the upper limit of the wavenumber range for 3- and 4-station circle arrays is the deviation wavenumber rk_d, beyond which the error term in the SPAC coefficient becomes dominant, while the upper limit for 5- and 9-station circle arrays is the wavenumber $rk = 3.2$ (equivalent to $\lambda = 2r$) assigned by Henstridge, beyond which the influence function is greatly magnified.

We are now able to see that what is important in estimating the SPAC coefficient to be used for analysis is either the deviation wavenumber, or the wavenumber range assigned by Henstridge (1979), both of which are dependent upon the number of stations.

As a result, we understand that all the upper limits of the wavenumber range thus assigned for various circle arrays do not exceed the wavenumber at which the SPAC coefficient takes its first minimum value. Up to this wavenumber the behaviour of the error due to a finite number of stations in the practical array is much the same as that due to infinite number of stations in the theoretical array, because the term $J_1(rk)$, as in the key equation (36), has the most noticeable effect on the behaviour of the influence function in equation (38).

We conclude that the 3-station circle array should be used as a very efficient practical circle array for the SPAC method, from which the SPAC coefficients can be estimated safely up to a frequency in the vicinity of the first minimum value of the SPAC coefficient. Increasing the number of stations to more than three on the circumference of a circular array increases field effort but may not always improve the analytical efficiency.

We should also consider the statistical consequences of using different numbers of stations. Increasing the number of stations can be expected to give a statistically better estimate of the SPAC coefficient in the specific wavenumber range. This is because

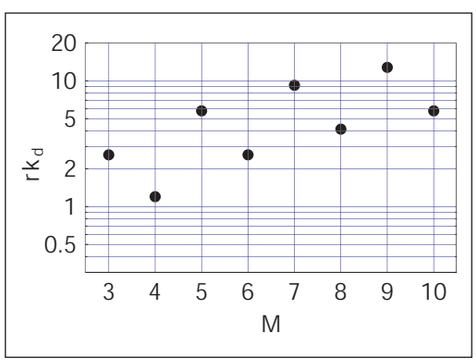

Fig. 5. Relationship between deviation wavenumer rk_d and the number of stations M on the circle of radius r, for practical circle arrays.

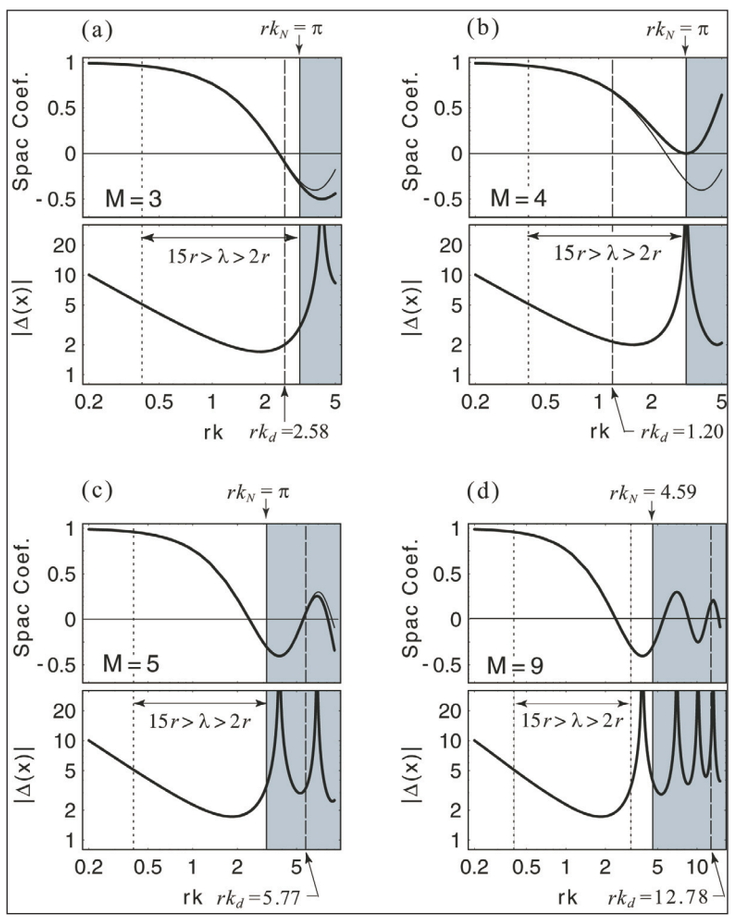

Fig. 6. The influence function $|\Delta(x)|$ in the error of SPAC coefficient due to the use of practical circle array of radius r (respective lower figures) and the SPAC coefficients (respective upper figures) for the four arrays shown in Figures (1)–(4). rk_d is the deviation wavenumber and rk_N the Nyquist wavenumber. The range indicated by arrows corresponds to the wavelength λ assigned by Henstridge (1979), outside which the error is greatly magnified. For wave components in the shaded area, aliasing occurs. Note that

if a value of the SPAC function (equation (32)), estimated from observed data, is assumed to be sampled from a normally distribution of values, then increasing the number of stations can provide statistically smaller variance of the SPAC function, which in turn provides a better estimate of the SPAC coefficient in the specific wavenumber range. For example, the SPAC coefficient estimated from a 6-station circle array (Asten, 2003; Asten, 2004; Roberts and Asten, 2004) must essentially be the same as that from a 3-station array, as shown by equation (33), but the variance of the coefficient estimated from the 6-station circle array would be expected to be smaller than that from the 3-station circle array. The maximum wavenumber for each array is limited to that wavenumber where the coefficient takes its first minimum value.

Spatial aliasing for an *M*-station circle array

When evaluating the SPAC coefficient to be estimated from an *M*-station circle array, spatial sampling should be examined as well. For sampling a continuous spatial data series as in our case, we need some sort of criterion to choose the spatial sampling interval Δl between any two points within the circle array. Incorrect sampling leads to some loss of information and this loss gets worse as Δl increases. However, making Δl very small increases field effort and decreases analytical efficacy. Hence, a compromise spatial sampling interval must be sought (e.g., Chatfield, 1989; Sheriff and Geldart, 1983).

Spatial sampling of data by the circle array may cause directional aliasing (Henstridge, 1979; Cho et al., 2004), or spatial aliasing in the estimation of the SPAC coefficient, but in practice, the effect of aliasing has rarely been discussed in the SPAC method. In our case we do not consider the effect of directional aliasing, because the SPAC coefficient that we estimate using an equally spaced *M*-station circle array is independent of the direction of arrival of microtremor energy because of the use of the equation of constraint (30). However, spatial aliasing must be considered. The discussion is limited to a simple case, because our main purpose is to consider comparative merits and demerits for the number of stations on a circle array.

Spatial sampling for the circle array is done at the shortest interval Δl between any two stations arbitrarily chosen from the array (Figure 7). This allows us to define the Nyquist wavenumber k_N as

$$k_N/2\pi = 1/2\Delta l\,, \tag{40}$$

which gives the maximum wavenumber per two sample intervals. When we have a wave component with a wavenumber k as $k > k_N$, aliasing occurs.

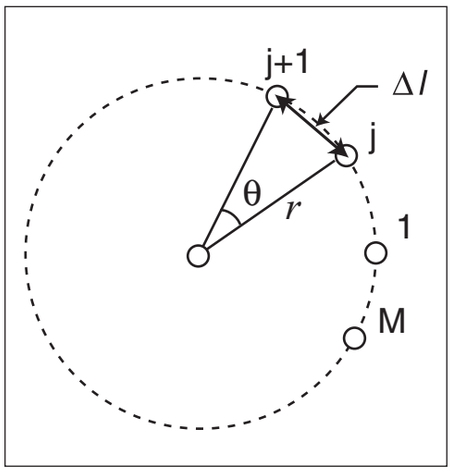

Fig. 7. The shortest distance between two stations in a circle array, $\Delta l = 2r\sin(\theta/2) = 2r\sin(\pi/M)$, for an *M*-station circle array ($M \geq 6$).

Since the sample interval Δl for an *M*-station circle array is given as

$$\Delta l = \begin{cases} r & \text{for} \quad M \leq 6, \\ 2r\sin(\pi/M) & \text{for} \quad M > 6, \end{cases} \tag{41}$$

the Nyquist wavenumber rk_N is

$$rk_N = \begin{cases} \pi & \text{for} \quad M \leq 6, \\ \pi/2\sin(\pi/M) & \text{for} \quad M > 6, \end{cases} \tag{42}$$

and the corresponding Nyquist frequency f_N is

$$f_N = ck_N/2\pi = \begin{cases} c/2r & \text{for} \quad M \leq 6, \\ c/4r\sin(\pi/M) & \text{for} \quad M > 6. \end{cases} \tag{43}$$

In Figure 6 the Nyquist wavenumber rk_N for each practical circle array is indicated, and the shaded areas indicate wavenumbers which would be aliased.

As is evident from equation (43), the Nyquist frequency f_N cannot be determined before the phase velocity c is determined at this frequency. This means that the Nyquist frequency and its corresponding phase velocity are essentially interdependent.

In practice it may be possible to estimate an "effective" Nyquist frequency in an iterative way using the following two steps: 1) SPAC coefficients over some frequency range are tentatively transformed to a phase velocity dispersion curve, assuming that wavenumber components may be spatially aliased at the Nyquist wavenumber. The phase velocity thus determined at a frequency at which the value of SPAC coefficient is almost equal to $J_0(rk_N)$ (for example, $J_0(\pi) = -0.3042\cdots$ for an *M*-station circle array with $M \leq 6$ from equation (42)) gives an effective Nyquist frequency f_N' by equation (43). A more desirable temporal sampling rate $\Delta t'$ can now be determined from $\Delta t' = 1/2f_N'$; that is, f_N' is a useful estimate for alias filtering. 2) Resampling at time interval $\Delta t'$ is done to reduce aliasing errors, and the SPAC coefficients are recalculated.

The Nyquist wavenumber rk_N for a 3-station circle array is π, from equation (42), and in Figure 6(a) we see that this is very close to but a little greater than the deviation wavenumber rk_d (= 2.58). This shows that the valid SPAC coefficient can safely be estimated up to the deviation wavenumber near which the theoretical SPAC coefficient takes its first minimum value.

Similarly, the Nyquist wavenumber for a 5-station circle array is also π, and that for a 9-station circle array, $\pi/2\sin(\pi/9)$ (≈ 4.59) from equation (42). In Figures 6(c) and 6(d) we see that the Nyquist wavenumber is fairly small compared with the deviation wavenumber for each array. This suggests that increasing the number of stations to 9 at most is not effective in extending the wavenumber range within which valid SPAC coefficients can be estimated. For example, the greatest wavenumber for which valid SPAC coefficients are available for a 9-station circle array is limited to $rk_N \approx 4.59$, which is fractionally greater than $rk_m \approx 3.83$ at which the SPAC coefficient takes its first minimum value, but there is the disadvantage that the error in the SPAC coefficient in the wavenumber range $rk_m < rk < rk_N$ may be greatly magnified, as is clearly seen in the lower part of Figure 6(d). Even for the 9-station circle array the upper limit of the wavenumber range in which the valid SPAC coefficient can be safely estimated is, at most, the wavenumber where the SPAC coefficient takes its first minimum value, which is not much different from the upper limit for the 3-station circle array.

To sum up this discussion, we can safely state that the Nyquist wavenumber plays the most important role in selecting an efficient practical circle array. In order to obtain the SPAC coefficients over a much wider wavenumber range, a combined array that is made up of many circular arrays with different radii should be used at a survey site. A 3-station circle array, which consists of the minimum number of circumferential stations, should be employed as the fundamental circular array. We conclude that the 3-station circle array is the most efficient practical circle array for the SPAC method.

CONCLUSIONS

We have developed a theory of efficient array observations of microtremors, with special reference to the spatial auto-correlation (SPAC) method. The method is used as a practical and useful tool that yields information on subsurface structure, using the following assumption: the vertical component of microtremors consists of surface (Rayleigh) waves, in which one mode (often the fundamental mode) is dominant. In the method one of the most important quantities to be derived from observed data is the SPAC coefficient. Rearranging the theoretical background of the method from an approach to the theory of stochastic processes, we find the theoretical SPAC coefficient to be equal to the Bessel function of the first kind $J_0(rk)$, but subject to the condition that observations were made with a continuous array of detectors on a circle of radius r.

We have derived an equation for the SPAC coefficient applicable to data obtained by a circular array consisting of a finite number of stations, in which M stations ($M \geq 3$) are placed at equal intervals on the circumference of a circle of radius r, with one further station at the centre of the circle (an M-station circle array). Using a constraint for the direction of waves propagating across the array (equation (30)), the equation could be expressed as the sum of two terms; the first term is the Bessel function $J_0(rk)$, which is the same as the SPAC coefficient derived for the theoretical circle array; the second term is expressed as a series of Bessel functions, which depend on the number of stations M in the circle array concerned.

The SPAC coefficient thus derived was numerically evaluated for four different arrays assumed: 3-, 4-, 5-, and 9-station circle arrays. For the evaluation, the deviation wavenumber was temporarily defined as the wavenumber beyond which the coefficient deviates from the theoretical one as wavenumber increases. The numerical examination showed that the deviation wavenumber increases as the number of stations increases, thus extending the wavenumber range over which the valid SPAC coefficient can be estimated.

Aliasing, an inherent property of circular arrays, has also been examined; the spatial sampling with an M-station circle array determines the Nyquist wavenumber for the array, which specifies the maximum wavenumber in the SPAC processing beyond which aliasing occurs. We found that the Nyquist wavenumber was almost equal to the deviation wavenumber for the 3-station circle array, and was fairly small in comparison with the respective deviation wavenumbers for both 5- and 9-station circle arrays, which suggests that increasing the number of stations on the circle to 9 is not very effective in extending the wavenumber range.

The evaluation gave the following results: 1) the Nyquist wavenumber due to spatial sampling for an M-station circle array is the most influential factor that definitely determines the upper limit of the frequency range over which a valid SPAC coefficient can be estimated; and 2) the 3-station circle array is the most favourable of those considered for efficient array observation of microtremors using the SPAC method, but with the condition that only the SPAC coefficients up to a frequency near which the coefficient takes its first minimum value should be employed.

ACKNOWLEDGMENTS

The careful reviews and helpful comments by Michael Asten and Adam O'Neill are greatly appreciated. I thank James Roberts for valuable comments, especially on the role of azimuthal direction on an earlier draft of this paper, and Koya Suto for reading the entire text in its original form and for his kind review that significantly improved this manuscript. Thanks are due to Kazuyoshi Kudo, Tsutomu Sasatani, Oguz Ozel, and Ling Suqun for frequent, stimulating, and helpful discussions.

REFERENCES

Aki, K., 1957, Space and time spectra of stationary stochastic waves, with special reference to microtremors: *Bulletin of the Earthquake Research Institute*, **35**, 415–456.

Aki, K., 1965, A note on the use of microseisms in determining the shallow structures of the earth's crust: *Geophysics*, **30**, 665–666.

Aki, K., Tsujiura, M., Hori, M., and Goto, K., 1958, Spectral study of near earthquake waves (1): *Bulletin of the Earthquake Research Institute*, **36**, 71–98.

Arfken, G.B., and Weber, H.J., 2001, *Mathematical Methods for Physicists* (5th edition): Academic Press.

Apostolidis, P., Raptakis, D., Roumelioti, Z., and Pitilakis, K., 2004, Determination of S-wave velocity structure using microtremors and spac method applied in Thessaloniki (Greece): *Soil Dynamics and Earthquake Engineering*, **24**, 49–67.

Asten, M.W., 2003, Lessons from alternative array design used for high-frequency microtremor array studies: in *Earthquake Risk Mitigation*, Wilson, J.L., Lam, N.K., Gibson, G.M., and Butler, B., Proceedings of a Conference of the Australian Earthquake Engineering Society, Melbourne, Paper No. 14.

Asten, M.W., 2004, Passive seismic methods using the microtremor wave field: *17th Geophysical Conference and Exhibition, Australian Society of Exploration Geophysicists, Extended Abstracts*.

Asten, M.W., 2005, *On bias and noise in passive seismic data from finite circular array data processed using SPAC methods*: (preprint).

Asten, M.W., and Henstridge, J.D., 1984, Array estimators and the use of microseisms for reconnaissance of sedimentary basins: *Geophysics*, **49**, 1828–1837.

Asten, M.W., Dhu, T., and Lam, N., 2004, Optimised array design for microtremor array studies applied to site classification; observations, results and future use: *Conference Proceedings of the 13th World Conference of Earthquake Engineering, Paper 2903*.

Capon, J., 1969, High-resolution frequency-wavenumber spectrum analysis: Proceedings of the Institute of Electrical and Electronics Engineers, **57**, 1408–1418.

Chatfield, C., 1989, *The Analysis of Time Series, an Introduction*, 4th edition: Chapman and Hall.

Cho, I., Tada, T., and Shinozaki, Y., 2004, A new method to determine phase velocities of Rayleigh waves from microseisms: *Geophysics*, **69**, 1535–1551.

Chouet, B., De Luca, G., Milana, G., Dawson, P., Martini, M., and Scarpa, R., 1998, Shallow velocity structure of Stromboli Volcano, Italy, derived from small-aperture array measurements of Strombolian tremor: *Bulletin of the Seismological Society of America*, **88**, 653–666.

Henstridge, J.D., 1979, A signal processing method for circular arrays: *Geophysics*, **44**, 179–184.

Hidaka, E., 1985, *Phase velocity of Rayleigh waves and S-wave velocity distribution estimated from long-period microtremors*: M.Sc. thesis (unpublished), Hokkaido University.

Horike, M., 1985, Inversion of phase velocity of long-period microtremors to the S-wave-velocity structure down to the basement in urbanized areas: *Journal of Physics of the Earth*, **33**, 59–96.

Hough, S.E., Seeber, L., Rovelli, A., Malagnini, L., DeCesare, A., Selveggi, G., and Lerner-Lam, A., 1992, Ambient noise and weak-motion excitation of sediment resonances: results from the Tiber Valley, Italy: *Bulletin of the Seismological Society of America*, **82**, 1186–1205.

Kudo, K., Kanno, T., Okada, H., Özel, O., Erdik, M., Sasatani, T., Higashi, S., Takahashi, M., and Yoshida, K., 2002, Site specific issues for strong ground motions during the Kocaeli, Turkey Earthquake of August 17, 1999, as inferred

from array observations of microtremors and aftershocks: *Bulletin of the Seismological Society of America*, **92**, 448–465.

Lacoss, R.T., Kelly, E.J., and Toksöz, M.N., 1969, Estimation of seismic noise structure using arrays: *Geophysics*, **34**, 21–38.

Malagnini, L., Rovelli, A., Hough, S.E., and Seeber, L., 1993, Site amplification estimates in the Garigliano Valley, central Italy, based on dense array measurements of ambient noise: *Bulletin of the Seismological Society of America*, **83**, 1744–1755.

Matsuoka, T., Umezawa, N., and Makishima, H., 1996, Experimental studies on the applicability of the spatial autocorrelation method for estimation of geological structures using microtremors: *Butsuri Tansa*, **49**, 26–41.

Matsuoka, T., and Shiraishi, H., 2002, Application of an exploration method using microtremor array observations for high resolution surveys of deep geological structures in the Kanto plains – Estimation of 3-D S-wave velocity structure in the southern part of Saitama prefecture : *Butsuri Tansa*, **55**, 127–143.

Matsushima, T. and Okada, H., 1989, A few remarks of the scheme of observation and analysis in estimating deep geological structures by using long-period microtremors: *Geophysical Bulletin of Hokkaido University*, **52**, 1–10.

Matsushima, T. and Ohshima, H., 1989, Estimation of underground structures using long-period microtremors – Kuromatsunai Depression, Hokkaido: *Butsuri Tansa*, **42**, 97–105.

Matsushima, T. and Okada, H., 1990, Determination of deep geological structures under urban areas: *Butsuri Tansa*, **43**, 21–33.

Miyakoshi, K., Okada, H., Sasatani, T., Moriya, T., Ling, S., and Saito, S., 1994, Estimation of geological structure under ESG blind prediction test sites in Odawara city by using microtremors: *Journal of the Seismological Society of Japan*, **47**, 273–285.

Miyakoshi, K., Okada, H., and Ling, S., 1996, Maximum wavelength possible to estimate phase velocities of surface waves in microtremors: *Proceedings of the 94th SEGJ Conference*, 178–182.

Morikawa, H., Sawada, S., and Akamatsu, J., 2004, A method to estimate phase velocities of Rayleigh waves using microseisms simultaneously observed at two sites: *Bulletin of the Seismological Society of America*, **94**, 961–976.

Nguyen, F., Rompaey, V., Teerlynck, H., Van Camp, M., Jongmans, D., and Camelbeeck, T., 2004, Use of microtremor measurement for assessing site effects in Northern Belgium –interpretation of the observed intensity during the Ms=5.0 June 11 1938 earthquake: *Journal of Seismology*, **8**, 41–56.

Okada, H., 1998, *Microtremors as an exploration method*: Geo-exploration Handbook, vol.2, Society of Exploration Geophysicists of Japan.

Okada, H., 2003, *The Microtremor Survey Method* (translated by Koya Suto): Geophysical Monograph Series, No.12, Society of Exploration Geophysicists.

Okada, H., and Sakajiri, N., 1983, Estimates of an S-wave velocity distribution using long-period microtremors: *Geophysical Bulletin of Hokkaido University*, **42**, 119–143.

Okada, H., Matsushima, T., and Hidaka, E., 1987, Comparison of spatial autocorrelation method and frequency-wavenumber spectral method of estimating the phase velocity of Rayleigh waves in long-period microtremors: *Geophysical Bulletin of Hokkaido University*, **49**, 53–62.

Okada, H., Matsushima, T., Moriya, T., and Sasatani, T., 1990, An exploration technique using long-period microtremors for determination of deep geological structures under urbanized areas: *Butsuri Tansa*, **43**, 402–417.

Okada, H., Matsuoka, T., Shiraishi, H., and Hachinohe, S., 2003, Spatial autocorrelation algorithm for the microtremor survey method using semicircular arrays: *Proceedings of the 109th SEGJ Conference*, 183–186.

Priestley, M.B., 1981, *Spectral Analysis and Time Series*: Academic Press.

Roberts, J.C., and Asten, M.W., 2004, Resolving a velocity inversion at the geotechnical scale using the microtremor (passive seismic) survey method: *Exploration Geophysics*, **35**, 14–18.

Roberts, J.C., and Asten, M.W., 2005, Estimating the shear velocity profile of Quaternary silts using microtremor array (SPAC) measurements: *Exploration Geophysics*, **36**, 34–40.

Sasatani, T. (Head Investigator), 2000, *Earthquake disaster evaluation based on estimation of deep underground structure and observation of strong ground motion in deep sedimentary basins*: A Report of the Study on Fundamental Science with Grant-in-Aid for Scientific Research (B)(2) by the Ministry of Education, No. 10480090, 164pp.

Sasatani, T., Yoshida, K., Okada, H., Nakano, O., Kobayashi, T., and Ling, S., 2001, Estimation of deep subsurface structures and observation of strong ground motions in Sapporo urban districts: J. JSNDS, **20**, 325–342.

Sheriff, R.E., and Geldart, L.P., 1983, *Exploration Seismology*, vol. 2: Cambridge University Press.

Watson, G.N., 1952, *A Treatise on the Theory of Bessel Functions* (2nd edition): Cambridge University Press.

Yaglom, A.M., 1962, *An introduction to the theory of stationary random functions* (translated and edited by R.A. Silverman): Dover Publications Inc.

Yamamoto, H., Iwamoto, K., Saito, T., and Yoshida, A., 1997, Discussion on sensor location in circular array for spatial autocorrelation method: *Proceedings of the 96th SEGJ Conference*, 444–447.

Yamanaka, H., Takemura, M., Ishida, H., Ikeura, T., Nozawa, T., Sasaki, T., and Niwa, M., 1994, Array measurements of long-period microtremors and estimation of S-wave velocity structure in the western part of the Tokyo metropolitan area: *Journal of the Seismological Society of Japan*, **47**, 163–172.

Yamanaka, H., Sato, H., Kurita, K., and Seo, K., 1999, Array measurements of long-period microtremors in southwestern Kanto plain, Japan, – Estimation of S-wave profiles in Kawasaki and Yokohama cities: *Journal of the Seismological Society of Japan*, **51**, 355–365.

微動アレイ観測のための空間自己相関法における効率的な観測点個数

岡田　廣[1]

要　旨：　S波速度の地下構造推定のために微動の鉛直成分のアレイ観測が行われる。観測データの取得，処理，解析には，よく空間自己相関法（略称：SPAC 法）が使われるが，観測のためには円の中心と円周上に有限個（M個）の観測点を配置した円形アレイ（略称：M点円形アレイ）が必要である。本論文では，解析効力を同じに保ち，野外の観測作業を効率的に行うには，円形アレイの周上に最小何個の観測点を配置すればよいか，という問題を論考した。

本論文では，まず SPAC 法の理論的背景を再整理し，“SPAC 係数”を定義した。それをもとに，1）円周上に隙間なく観測点を無限個配置した場合の“理論 SPAC 係数”は，アレイ半径 r と波数 k に依存する第 1 種 0 次のベッセル関数 $J_0(rk)$ で表せる，2）M点円形アレイの場合の SPAC 係数は，“理論 SPAC 係数”と，付加項すなわち，微動源の項を含まない，アレイ半径 r，波数 k，円周上の観測点数Mを変数とするベッセル1関数の無限級数との和で表される，ことなどを導いた。付加項は SPAC 係数の誤差に相当する。実際の観測を想定し，誤差の項の波数による変化を考察した。また，空間エイリアシングに起因する円形アレイに固有のナイキスト波数についても考察した。

これより，微動アレイ観測に対する SPAC 法の適用について，1）波数の増加とともに一見周期的に変化する SPAC 係数の値を，最初の極小値となる波数まで使うという条件の下では，円周上 3 観測点の円形アレイが最も効率的であること，2）SPAC 係数を推定する場合，その波数領域の上限を規定する因子はナイキスト波数であること，などの結果を得た。

キーワード：微動探査、レイリー波、ベッセル関数、円形アレイ、SPAC 係数

SPAC 방법에 근거한 상시진동의 효과적 배열 관측 이론

Hiroshi Okada[1]

요　약：　상시진동의 수직 성분에 대한 배열 관측은 상시진동이 대부분 레일리파의 기본 모드로 이루어졌다는 가정하에 지하 층서구조를 추정하기 위해 자주 수행된다. 자료획득, 처리 및 분석의 유용한 도구로서 공간자기상관(SPAC) 방법이 많이 사용되는데 이는 실제로 M 개의 원형 수진기 배열과 중앙의 하나 측점으로 이루어진다 (M 측점 원형 배열). 이 논문에서는 분석 효율 및 현장 노력의 관점에서 효율적인 자료획득을 위한 원형 배열에 필요한 측점의 최소 수에 대해 연구하였다.

이 연구에서는 먼저 M 무한대의 원형 배열을 위한 SPAC 계수들이 단지 Bessel 함수 J0(rk)(r 은 반지름, k 는 파수)로서 표현되는 SPAC 알고리듬의 이론적 배경을 재정리하였다. 두번째로 M 측점 원형 배열에 대해 상시진동 에너지장과 무관한 오차항을 포함하는 SPAC 계수들을 배열을 가로지르는 파의 방향에 한해 해석적으로 유도해 내고 수치적으로 이들 오차항들에 대해서 평가하였다. 주요 평가 결과들은: 1) 만약 SPAC 계수들이, 계수가 첫번째 최소값을 갖는 주파수까지 이용되면 다른 4-, 5-, 9-측점 배열들에 비교했을 때 3-측점 원형배열이 상시진동의 관측에 효율적이고 유리하다. 2) 나이퀴스트 파수가 유효한 SPAC 계수가 평가될 수 있는 주파수의 상한선을 결정하는데 가장 영향을 끼치는 요소이다.

주요어：상시진동 탄성파 탐사법, 레일리파, Bessel 함수, 효율적인 원형배열, SPAC 계수

1 産業技術総合研究所　地質情報研究部門
〒305-8567 茨城県つくば市東 1-1-1 中央第 7

1 산업기술종합연구소 지질정보연구부문